

# Effects of Metallic Gates on ac Measurements of the Quantum Hall Resistance

Frédéric Overney, Blaise Jeanneret and Beat Jeckelmann \*

June 1, 2022

## Abstract

Using a sample with a split back-gate, a linear frequency dependence of the ac quantum Hall resistance was observed. The frequency coefficient, which is due to dielectric losses produced by leakage current between the 2DEG and the back-gates, can be turned from a positive to a negative values by increasing the back-gate voltage. More interestingly, by removing these back-gates, the losses can be considerably reduced leading to a residual frequency coefficient on the order of  $(0.03 \pm 0.03) \cdot 10^{-6} / \text{kHz}$ . Moreover, at 1 kHz, an extremely flat plateau was observed over a magnetic field range of 1.4 T. These results clearly indicate that the audio frequency dependence of the QHR is to a large extent related to the measurement apparatus and does not originate from the physical transport properties of the 2DEG.

## 1 Introduction

The universal nature of dc electron transport in a two dimensional electron gas (2DEG) at low temperature and high magnetic field makes the quantum Hall resistance (QHR) an ideal primary standard of resistance (see [1] for the latest review on the application of the quantum Hall effect in metrology).

The situation in the regime of ac transport is rather different. The pioneering work of Melcher [2] showed that the QHR measured at a frequency of 1592 Hz agrees with  $R_K/2$  ( $R_K \equiv h/e^2$  is the von Klitzing constant) with a relative standard uncertainty of  $3 \mu\Omega/\Omega$ . This work has triggered a series of investigations at several National Metrology Institutes. Although various controversial results have been obtained, a few common features were observed [1]: the plateaus in the quantum Hall resistance  $R_H$  are no longer as flat and broad as they are at dc. In addition, the QHR has a linear frequency dependence caused by losses along the sample edges due to the presence of metallic gates in the vicinity of the 2DEG [3, 4].

---

\*The authors are with the Swiss Federal Office of Metrology and Accreditation, Lindenweg 50, CH-3003 Bern-Wabern, Switzerland (e-mail: frederic.overney@metas.ch).

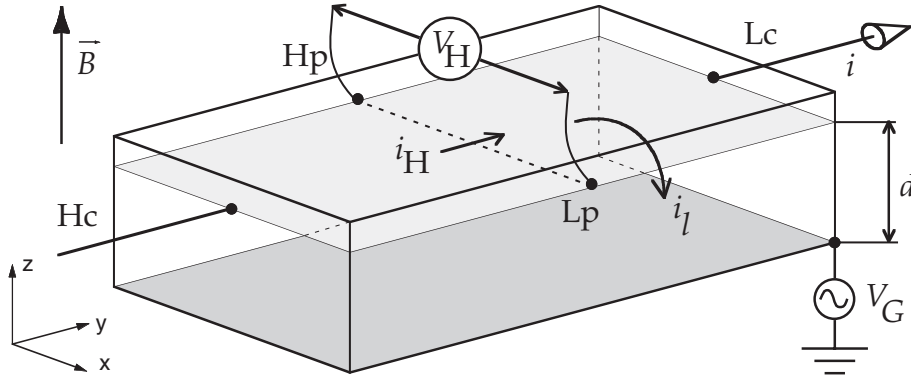


Figure 1: Schematic of a AlGaAs/GaAs heterostructure showing the loss mechanism due to the capacitive current flowing from the 2DEG to the back-gate.

In this paper, we show that, by removing metallic gates from the vicinity of the sample, the frequency dependence of the QHR can be strongly reduced without any external potential adjustment. Under appropriate conditions, the losses can be reduced to a level where the ac QHR can be used as an ac resistance standard with an uncertainty of a few parts in  $10^8$  at kHz frequencies over a magnetic field range broader than 1 T. These results suggest that the frequency dependence observed in earlier ac measurements of the QHR originate to a large extent in the measurement apparatus and not in the physical properties of the 2DEG.

## 2 Model for ac Losses

In figure 1, a two-dimensional electron gas (2DEG), located in a AlGaAs/GaAs heterostructure is sketched. The current, directed along the y-axis, enters the 2DEG through the contact  $H_c$  and leaves it through the contact  $L_c$ . For a magnetic field directed along the z-axis, the low and high potential contacts are  $H_p$  and  $L_p$  respectively. A back-gate is located at a distance  $d$  underneath the 2DEG and kept at a potential  $V_G$ . The Hall impedance  $Z_H$  of the device is defined by the ratio of the Hall potential  $V_H$ , measured between the potential contacts  $H_p$  and  $L_p$ , to the current  $i$  leaving the device at the current contact  $L_c$ . In this model, the deviation of  $Z_H$  from the Hall resistance  $R_H$  is due to leakage current. More precisely, the current  $i$  leaving the device at  $L_c$  is not equal to the Hall current  $i_H$  generating the Hall voltage because a small capacitive leakage current  $i_l$  flows to the backgate and does not contribute to  $i$ . Therefore, considering that  $V_H = R_H i_H$ :

$$Z_H = \frac{V_H}{i} = \frac{V_H}{i_H - i_l} \approx R_H \left(1 + \frac{R_H}{V_H} i_l\right) = R_H (1 + \Delta) \quad (1)$$

Considering that each elementary surface,  $dx dy$ , of the 2DEG forms a parallel plate capacitor with the back-gate, the leakage current  $i_l$  can be expressed as

$$i_l = j\omega\tilde{\epsilon}V_H\frac{\epsilon_o}{d}\iint_S\left(\frac{V(x,y)-V_G}{V_H}\right)dx dy \quad (2)$$

$$= j\omega\tilde{\epsilon}C_o(B,V_G)V_H \quad (3)$$

where  $j = \sqrt{-1}$ ,  $\omega = 2\pi\nu$  is the angular frequency,  $\tilde{\epsilon}$  is the complex dielectric constant of the heterostructure,  $\epsilon_o$  is the permittivity of free space and  $V(x,y)$  is the local potential of the 2DEG. The term  $C_o(B,V_G)$  can be interpreted as the equivalent free space capacitance between the 2DEG and the backgate. It is not a purely geometrical capacitance but rather an electrochemical capacitance in the sense of [5]. Therefore, if the potential of the backgate is sufficiently high, the sign of the current is inverted and an extra current is now injected in the 2DEG from the backgate. Accordingly,  $C_o(B,V_G)$  is then negative.

The integration surface  $S$  extends from the line between the potential contacts,  $H_p$  and  $L_p$  and the sample edge where the current leaves the 2DEG through the  $L_c$  contact. Any current flowing between the 2DEG and the backgate before the potential contact does not induce any error. Indeed, if a leakage current leaves the 2DEG before the potential contact, it will neither generate a Hall voltage nor contribute to the current  $i$ . Similarly, if a current is injected into the 2DEG from the backgate before the potential contacts, it will generate an Hall voltage and also contribute to the current  $i$ .

The leakage current  $i_l$  is mostly in quadrature with the Hall current  $i_H$ , however, dielectric losses in the GaAs heterostructure will generate a small in-phase component. Writing the complex dielectric constant as  $\tilde{\epsilon} = \epsilon(1 - j\tan(\delta))$ ,  $\epsilon$  being the real component of the dielectric constant and  $\tan(\delta)$  the dielectric losses, the correction term  $\Delta$  in (1) becomes

$$\Delta = \omega R_H\epsilon\tan(\delta)C_o(B,V_G) + j\omega R_H\epsilon C_o(B,V_G) \quad (4)$$

The loss mechanisms introduce a linear frequency dependence in  $\Re\{Z_H\}$  that can be reduced by making  $C_o(B,V_G)$  as small as possible.

### 3 The ac bridge and the connection scheme

The ac quantum Hall effect was investigated by measuring the ratio between  $Z_H$  measured on the plateau  $i = 2$  and a quadrifilar resistor  $Z_G$  of the same nominal value having a calculable ac/dc difference [6].

Figure 2 shows the schematic of the bridge constructed according to the usual ac coaxial bridge techniques [7]. For simplicity, the outer coaxial conductor is omitted. The bridge is powered by the double screened transformer  $T_S$  featuring taps with output voltages equal to  $\pm 2U$ ,  $\pm U$ ,  $\pm U/2$  and 0, where  $U$  is the nominal voltage applied to the QHR and to  $R_G$ . The Wagner autotransformer  $T_W$  is used to compensate the leakage current until the load current  $i_0$  at the centre tap of the ratio autotransformer  $T_R$  is zero. The combining network

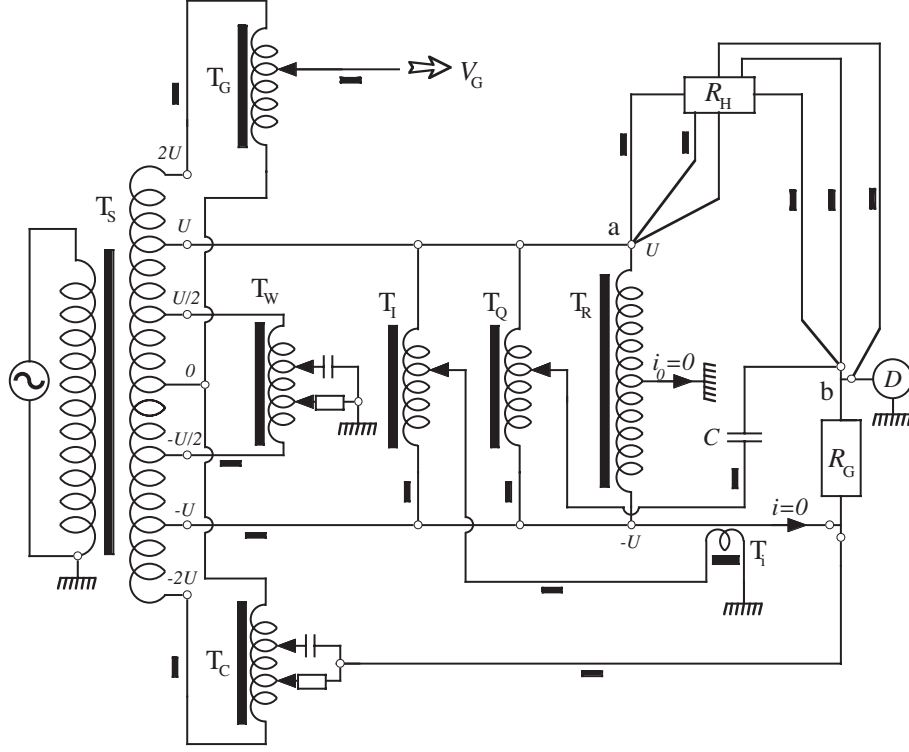


Figure 2: Schematic of the ac bridge.

$T_C$  acts as a current source and is adjusted to zero the current  $i$  through the lead between the high potential port of  $R_G$  and the  $-U$  tap of  $T_R$ . The ratio of the resistors has a small deviation from unity that is compensated using the autotransformer  $T_I$  and the injection transformer  $T_I$  for the in-phase component, and using the autotransformer  $T_Q$  and the low loss capacitor  $C$  for the quadrature component. The offset of the 1:1 ratio of the autotransformer  $T_R$  is measured by repeating the comparison with  $T_R$  reversed. Finally, the autotransformer  $T_G$  sets the potential  $V_G$  of the back gate when gated samples are measured. The quantum Hall sample is connected to the bridge using a multiple series connection [8]. In such a connection scheme, the current and potential leads of the same polarity are tied together at the external junction points a and b where the apparent quantum Hall impedance  $Z_H$  can be defined as a two terminal-pair component  $Z'_H$ . The quadrifilar resistor  $Z_G$  is defined as a four terminal-pair component  $Z'_G$ . Accounting for cable correction one obtains [9, 4]

$$\begin{aligned}
 Z'_H &= Z_H \cdot \left(1 + \frac{Y_{H_p} Z_{H_p}}{2}\right) \cdot \left(1 + \frac{Y_{L_c} Z_{L_c}}{2}\right) \\
 &\quad \cdot \left(1 + \left(\frac{Z_{H_p}}{Z_H}\right)^n + \left(\frac{Z_{L_c}}{Z_H}\right)^m\right)
 \end{aligned} \tag{5}$$

$$Z'_G = Z_G \cdot \left(1 + \frac{Y_{H_p} Z_{H_p}}{2}\right)^{-1} \cdot \left(1 + \frac{Y_{L_c} Z_{L_c}}{2}\right)^{-1} \quad (6)$$

where the terms  $YZ = \omega^2 LC + j\omega RC$  are related to the leads which define the high potential (index  $H_p$ ) and the low current (index  $L_c$ ). The cable corrections are dominated by the terms involving the long coaxial cables linking the quantum Hall device, inside the cryostat, to the junction points a and b outside the cryostat. The real component of the total cable correction is proportional to the square of the frequency and amounts to  $9.2 \cdot 10^{-8}/\text{kHz}^2$ .

The exponents  $n$  and  $m$  in (5) are related to the multiple series connection scheme and denote the number of leads connected to the high- and low-junction points (a and b respectively).

## 4 Experimental Results and Discussions

Measurements have been carried out on three GaAs heterostructures (Type LEP 514 [10]). The first device, LEP1, is mounted on a printed circuit board equipped with a classical back-gate connected to the shield. The second device, LEP2, is mounted on a printed circuit board equipped with a split back-gate in a way similar to [11]. While the back-gate underneath the low potential side of the QHR was always grounded, the potential of the back-gate below the high potential side was set to a potential  $V_G$  ranging between 0 and  $2V_H$  using the autotransformer  $T_G$ . The third device, LEP3, is mounted on a printed circuit board where the back-gate was removed and all metallic parts were kept as far as possible from the sample. At a temperature of 0.3 K, the frequency dependence of the Hall impedance  $Z_H$  on the plateau  $i = 2$  was investigated with an ac current of 20  $\mu\text{A}$ . The frequency was varied between 800 Hz and 5 kHz.

### 4.1 Changing the Position of the Potential Contact

The frequency dependence of the Hall impedance of the sample LEP1 in three different double-series connections is shown in Fig.3 (solid symbols) for three different pairs of potential contacts.

A linear frequency dependence is observed in the real component of  $Z_H$ . For the configuration A the linear frequency coefficient  $\alpha \equiv \partial \Re\{Z_H\}/\partial \nu$  amounts to  $0.53 \cdot 10^{-6}/\text{kHz}$  and decreases to  $0.28 \cdot 10^{-6}/\text{kHz}$  for the configuration C. The linear frequency coefficient  $\beta \equiv \partial \Im\{Z_H\}/\partial \nu$  shows a similar behaviour.

As expected from our model, the total leakage current  $i_l$  decreases when the potential contacts are moved toward  $L_c$ , i.e. the integration surface  $S$  decreases, therefore reducing the linear frequency coefficient,  $\alpha$  and  $\beta$ . The variation of  $\alpha$  (respectively  $\beta$ ) as a function of the distance between the potential contacts and  $L_c$  is close to linear. This means that the equivalent free space capacitance  $C_o$  is quite homogeneously distributed along the sample at least in the central part of the device, i.e. far from the current contacts. According to (4), the ratio of these variation rates gives an estimation of the loss factor  $\tan(\delta)$ . Our measurement leads to a loss factor of 0.02, which is four times larger than the

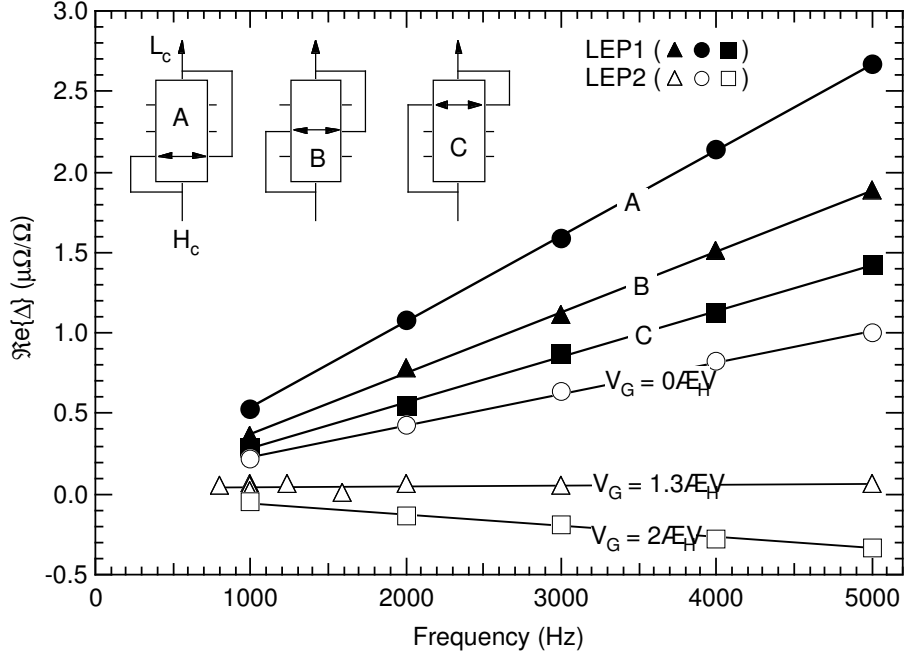


Figure 3: Relative deviation of the real component of  $Z_H$ ,  $R_H(1 + \Re\{\Delta\})$ , from its extrapolated DC value,  $R_H$ , measured at  $20 \mu\text{A}$  on the centre of plateau  $i=2$  of two different samples. Solid symbols: LEP1 using the three different double-series connections showed in the inset (the magnetic field points out of the page). Open symbols: LEP2 applying three different voltages to the back-gate, the sample being connected with the triple series-connection.

loss factor of GaAs (0.005) [12]. However, it agrees very well with values (0.02-0.03) derived from conductance and capacitance measurements carried out on a similar heterostructure [3].

## 4.2 Changing the Potential of the Gates

The frequency dependence of both  $\Re\{Z_H\}$  and  $\Im\{Z_H\}$  has been measured on the LEP2 device for three different settings of the back-gate potential  $V_G$ : at ground, at twice the Hall voltage and at a potential adjusted to zero the current coefficient according to the procedure described in [11]. Figure 3 shows the relative variation of  $\Re\{Z_H\}$  with the frequency at three different back-gate voltages (open symbols). As expected, the linear frequency coefficient  $\alpha$  decreases when the gate potential is increased. For the gate voltage of  $2V_H$ ,  $\alpha$  becomes negative meaning that the current  $i_i$  is now flowing from the back-gate to the 2DEG. The value of the potential leading to a zero frequency coefficient is slightly above the Hall voltage ( $V_G = 1.3V_H$ ).

The variation of the frequency coefficients,  $\alpha$  and  $\beta$ , is linear as a function

of the back-gate voltage. The ratio of the slopes of this linear gate voltage dependence gives again an estimation of the loss factor of the heterostructure. Our measurement leads to a value of 0.015 which is consistent with the value of 0.02 previously obtained.

### 4.3 Removing the Gates

Figure 4 shows the frequency dependence of  $\Re\{Z_H\}$  measured on the ungated device LEP3 using an asymmetric multiple-series connection (A) and a triple-series connection (B). In both cases, a small residual linear frequency coefficient of  $(0.03 \pm 0.03) \cdot 10^{-6}/\text{kHz}$  is still observed. As predicted by our model, the leakage current is strongly reduced by removing the back-gate. At the moment, it is not clear whether this slope comes from a residual leakage current between the 2DEG and some metallic parts around the sample or from any intrinsic properties of the 2DEG, like for example, the capacitance associated with the edge states [13]. An additional difficulty in modelling losses in the 2DEG occurs at the corners of the device where the current is injected/extracted from the 2DEG. These hot spots where a large potential drop takes place over a short distance could also play a role in the residual frequency dependence observed in Fig.4.

While  $\Re\{Z_H\}$ , measured with the triple-series connection (B), converges effectively to  $R_K/2$  at zero frequency, the value obtained with the asymmetric multiple-series connection (A) differs by  $0.2 \cdot 10^{-6}$ . We attribute this deviation to the cable correction term  $(Z/Z_H)^2 = 0.48 \cdot 10^{-6}$  in eq. 5 for which we use the room temperature resistance value of the cable ( $9 \Omega$ ). Therefore, the calculated correction is slightly overestimated and a  $-0.2 \mu\Omega/\Omega$  offset is observed at zero frequency. For the measurements carried out using the asymmetric multiple-series connection (A), a deviation from the linear frequency dependence is clearly visible at 2 kHz. Such a resonance has already been observed [9] and is attributed to vibrations of the bonding wires. Therefore, we excluded the values measured at frequencies 1592 Hz, 2000 Hz and 2500 Hz from the linear fit. Such a peak does not appear in the triple-series connection (B) measurements. Either the resonance frequency of the bonding wires is out of the frequency range or the peak amplitude, which is damped by a factor  $(1/R_H)^3$ , is too small to be observed.

Figure 5 shows the shape of the plateau  $i = 2$  measured on LEP3 in the asymmetric multi-series connection at 1 kHz and 5 kHz. The sweep was carried out step by step and each value is the average of a one minute measurement. The plateau at 1 kHz is remarkably flat with a peak-to-peak ripple of only of  $0.04 \cdot 10^{-6}$  over a field range larger than 1.4 T. At 5 kHz, the peak-to-peak ripple amounts to  $0.12 \cdot 10^{-6}$  over the same field range. A small feature is present in the high-B side of the plateau, which is related to a geometrical effect [14]. Indeed, due to the finite width of the voltage probes, a small component of the longitudinal resistance is mixed into the Hall resistance. Otherwise, we did not observe a significant variation of the plateau width up to the frequency of 5 kHz.

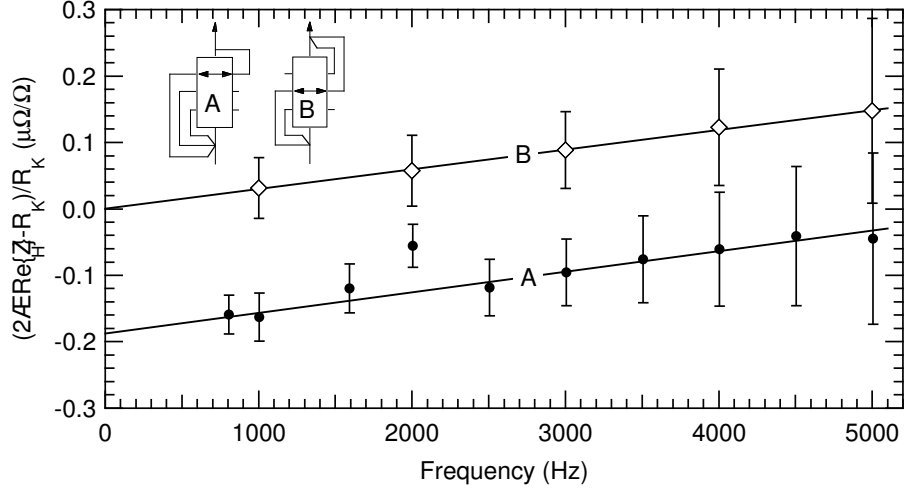


Figure 4: Relative deviation of  $Re\{Z_H\}$  from  $R_K/2$  measured on the ungated LEP3 sample. The uncertainty bars correspond to  $1\sigma$ .

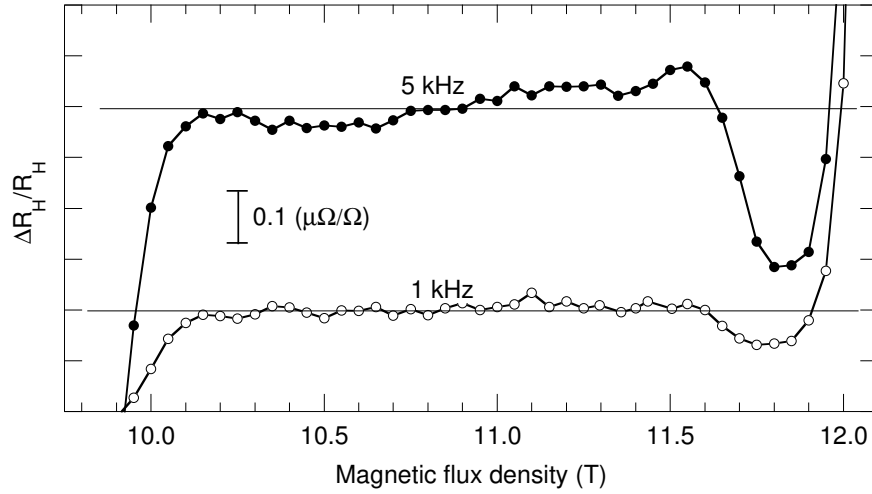


Figure 5: Shape of the plateau  $i = 2$  measured on LEP3 with the asymmetric multi-series connection (see configuration A in Fig. 3 at 1 kHz and 5 kHz). An offset between the two curves has been added for clarity. The horizontal lines are a guide to the eye.



## 5 Conclusion

According to a phenomenological model, the linear frequency dependence observed with gated quantum Hall samples can be attributed to dielectric losses produced by leakage currents between the 2DEG and the back-gate. This model also explains the effect of the back gate potential on the slope of the frequency coefficient. In a different experiment, the leakage currents were severely suppressed by simply removing the back-gate. In this case, a residual frequency coefficient of  $(0.03 \pm 0.03) \cdot 10^{-6}/\text{kHz}$  was obtained without any external potential adjustment. Here we want to strongly emphasise that this absence of potential adjustment is particularly important in view of using the ac quantum Hall effect as a primary standard of ac resistance. In addition, the ungated sample exhibits a broad (around 1.4 T wide) and flat (ripple of 4 parts in  $10^8$ ) plateau making the QHR suitable for high precision ac metrological applications. Finally, these results suggest that the frequency dependence observed in many experiments originates to a large extent in the measurement apparatus and not in the physical properties of the 2DEG.

## 6 Acknowledgments

The authors would like to acknowledge F. Delahaye for the supply of LEP devices and H. Bärtschi for his skillful assistance.

## References

- [1] B. Jeckelmann and B. Jeanneret, “The quantum Hall effect as an electrical resistance standard,” *Rep. Prog. Phys.*, vol. 64, pp. 1603–1656, 2001.
- [2] J. Melcher, P. Warnecke, and R. Hanke, “Comparison of precision ac and dc measurements of the quantized Hall resistance,” *IEEE Trans. Instrum. Meas.*, vol. 42, pp. 292–294, 1993.
- [3] F. Delahaye, B. Kibble, and A. Zarka, “Controlling ac losses in quantum Hall effect devices,” *Metrologia*, vol. 37, pp. 659–670, 2000.
- [4] J. Schurr, J. Melcher, A. von Campenhausen, K. Pierz, G. Hein, and F.-J. Ahlers, “Loss phenomena in the AC quantum Hall effect,” *IEEE Trans. Instrum. Meas.*, vol. 50, pp. 214–217, 2001.
- [5] T. Christen and Büttiker, “Low frequency admittance of quantized Hall conductors,” *Phys. Rev. B*, vol. 53, pp. 2064–2072, 1996.
- [6] D. Gibbings, “A design for resistors of calculable a.c./d.c. resistance ratio,” *Proc. IEE*, vol. 110, pp. 335–347, 1963.
- [7] B. Kibble and G. Rayner, *Coaxial ac bridges*. Bristol: Adam Hilger Ltd, 1984.

- [8] F. Delahaye, “Series and parallel connection of multiple quantum Hall-effect devices,” *J. Appl. Phys.*, vol. 73, pp. 7914–7920, 1993.
- [9] S. Chua, A. Hartland, and B. Kibble, “Measurement of the ac quantized Hall resistance,” *IEEE Trans. Instrum. Meas.*, vol. 48, pp. 309–313, 1999.
- [10] F. Piquemal, G. Genevès, F. Delahaye, J.-P. André, J.-N. Patillon, and P. Frijlink, “Report on a joint BIPM-EUROMET project for the fabrication of QHE samples by the LEP,” *IEEE Trans. Instrum. Meas.*, vol. 42, pp. 264–268, 1993.
- [11] F. Delahaye, “Instructions for ac measurements of gated QHE devices,” Bureau International des Poids et Mesures, Paris, vol. 1, pp. 1–11, 2001.
- [12] G. Samara, “Temperature and pressure dependences of the dielectric constants of semiconductors,” *Phys. Rev. B*, vol. 27, pp. 3494–3505, 1983.
- [13] B. Jeanneret, B. Jeckelmann, and B. Hall, “Contactless measurements of the internal capacitance of a Corbino ring in the quantum Hall regime,” *IEEE Trans. Instrum. Meas.*, vol. 48, pp. 301–304, 1999.
- [14] W. van der Wel, C. Harmans, and J. Mooij, “A geometric explanation of the temperature dependence of the quantised Hall resistance,” *J. Phys. C*, vol. 21, pp. L171–L175, 1988.